Available on CMS information server

**CMS NOTE 2011/XXX**

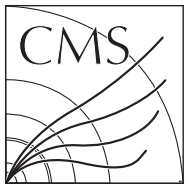

**The Compact Muon Solenoid Experiment**

# CMS Note

Mailing address: CMS CERN, CH-1211 GENEVA 23, Switzerland

**May 28, 2013**

# $\mathrm{E}_{\mathrm{T}}^{\mathrm{miss}}$ Templates Results and Additional Cross-checks for the Opposite-sign Same-flavor ("Edge") Dilepton Analysis

D. Barge, A. George, C. Campagnari, F. Golf, J. Gran, D. Kovalskyi, V. Krutelyov

*University of California, Santa Barbara, USA*

G. Cerati, D. Evans, R. Kelley, I. MacNeill, S. Padhi, Y. Tu, F. Würthwein, V. Welke, A. Yagil, J. Yoo

*University of California, San Diego, USA*

L. Bauerdick, K. Burkett, I. Fisk, Y. Gao, O. Gutsche, B. Hooberman, S. Jindariani, J. Linacre, V. Martinez Outschoorn

*Fermi National Accelerator Laboratory, Batavia, Illinois, USA*

**Abstract**

The Aachen and ETH groups have reported an excess of events with low mass, opposite-sign same-flavor lepton pairs, commonly referred to as the "edge analysis." In this note, we use the $\mathrm{E}_{\mathrm{T}}^{\mathrm{miss}}$ templates technique to estimate the Z background in the Z mass region for the four signal regions used in this analysis. This prediction is extrapolated to low mass to estimate the $\gamma^*/Z$ contribution. Additional cross-checks are also presented.

# Contents

# 1 Changes since previous version

- AN v2: Update the selection. For the high-$\mathrm{E_T^{miss}}$ signal region require both leptons to satisfy $p_T > 20$ GeV (previously the trailing lepton $p_T$ threshold was 10 GeV). For both the low-$\mathrm{E_T^{miss}}$ and high-$\mathrm{E_T^{miss}}$ signal regions, we now quote the results in the "central region" and "inclusive region" defined by requiring both leptons to satisfy $|\eta| < 1.4$ and $|\eta| < 2.4$, respectively (4 total signal regions).

# 2 Introduction

The Aachen and ETH groups have reported an excess of events with low mass, opposite-sign same-flavor (OSSF) lepton pairs, as described in AN-2012/200 (Aachen) and AN-2012/231 (ETH). In Sec. 3 we define the signal regions used in the analysis and demonstrate the level of synchronization with the ETH and Aachen authors. In Sec. 4 of this note, we use the $\mathrm{E_T^{miss}}$ templates technique [1] to estimate the Z background in the Z mass region for the two signal regions used in this analysis. This prediction is extrapolated to low mass to estimate the $\gamma^*/Z$ contribution. In Sec. C we cross-check the results of the nominal analysis based on dilepton triggers using single lepton triggers. **All results presented here are based on 9.2 fb$^{-1}$.**

# 3 Signal Regions and Synchronization Exercise

We begin by defining the signal regions used in the edge analysis, and demonstrating the level of synchronization with the results from the ETH and Aachen authors.

## 3.1 Signal Regions

The signal regions of the OSSF analysis are defined as:

- Low-$\mathrm{E_T^{miss}}$ signal region (ETH)
  - At least 3 jets ($p_T > 40$ GeV, $|\eta| < 3$)
  - $\mathrm{E_T^{miss}} > 100$ GeV
  - 2 $p_T > 20$ GeV leptons with $|\eta| < 1.4$ (central leptons) or $|\eta| < 2.4$ (inclusive leptons)
- High-$\mathrm{E_T^{miss}}$ signal region (Aachen)
  - At least 2 jets ($p_T > 40$ GeV, $|\eta| < 3$) with scalar sum $H_T > 100$ GeV
  - $\mathrm{E_T^{miss}} > 150$ GeV
  - 2 $p_T > 20$ GeV leptons with $|\eta| < 1.4$ (central leptons) or $|\eta| < 2.4$ (inclusive leptons)

This gives a total of four signal regions: low-$\mathrm{E_T^{miss}}$ central, low-$\mathrm{E_T^{miss}}$ inclusive, high-$\mathrm{E_T^{miss}}$ central, and high-$\mathrm{E_T^{miss}}$ inclusive. The edge signal regions are defined by requiring the lepton pair to have $20 < m_{\ell\ell} < 70$ GeV ("low-mass"), in this note we also examine the results in the $81 < m_{\ell\ell} < 101$ GeV ("on-Z") region.

## 3.2 Synchronization Exercise

We perform a synchronization exercise to make sure that we can reproduce the ETH/Aachen results. In Table 1 we compare our on-Z yields with those from the Aachen and ETH groups. In Table 2 we compare our low-mass yields with those from the Aachen and ETH groups. In general we are synchronized to within a few% in all channels.

Table 1: Summary of the synchronization exercise for the on-Z yields, obtained from the ETH/Aachen authors via private communication. The yields in the on-Z region are displayed for the low $\mathrm{E_T^{miss}}$ central and high $\mathrm{E_T^{miss}}$ inclusive signal regions.

| low $\mathrm{E_T^{miss}}$ signal region (central) | UCSB-UCSD-FNAL | ETH Authors |
|---|---|---|
| ee | 91 | 89 |
| $\mu\mu$ | 102 | 102 |
| e$\mu$ | 130 | 130 |
| high $\mathrm{E_T^{miss}}$ signal region (inclusive) | UCSB-UCSD-FNAL | Aachen |
| ee | 61 | 60 |
| $\mu\mu$ | 73 | 78 |
| e$\mu$ | 95 | 94 |

Table 2: Summary of the synchronization exercise comparing with Table 4 of SUS-12-019 v9. The yields in the low-mass region are displayed for the low $\mathrm{E_T^{miss}}$ and high $\mathrm{E_T^{miss}}$ signal regions, in the central and inclusive regions. The opposite-flavor prediction (OF) is the number of e$\mu$ events scaled by $R_{SF/OF} = 1.02$.

| low $\mathrm{E_T^{miss}}$ signal region (central) | UCSB-UCSD-FNAL | SUS-12-019 v9 Table 4 |
|---|---|---|
| SF | 364 | 364 |
| OF | 265 | 264 |
| low $\mathrm{E_T^{miss}}$ signal region (inclusive) | UCSB-UCSD-FNAL | SUS-12-019 v9 Table 4 |
| SF | 453 | 452 |
| OF | 368 | 367 |
| high $\mathrm{E_T^{miss}}$ signal region (central) | UCSB-UCSD-FNAL | SUS-12-019 v9 Table 4 |
| SF | 168 | 174 |
| OF | 114 | 119 |
| high $\mathrm{E_T^{miss}}$ signal region (inclusive) | UCSB-UCSD-FNAL | SUS-12-019 v9 Table 4 |
| SF | 217 | 222 |
| OF | 149 | 154 |

# 4 Results of the $\mathrm{E_T^{miss}}$ Templates Analysis

In this section, we use the $\mathrm{E_T^{miss}}$ templates technique to derive predictions for the background in the on-Z region for the four signal regions used for the edge analysis. The background estimation methodology used in the $\mathrm{E_T^{miss}}$ templates analysis is described in AN-2012/254; this AN presents only details which differ from that reference. We then use the predicted Z background to derive an estimate of the low-mass $\gamma^*$/Z contribution, using an extrapolation technique commonly referred to as the "$R_{out/in}$" technique [2].

## 4.1 Background Estimation Methodology

The strategy is to select Z$\rightarrow \ell\ell$ candidates ($81 < m_{\ell\ell} < 101$ GeV) with jet requirements corresponding to the low-$\mathrm{E_T^{miss}}$ and high-$\mathrm{E_T^{miss}}$ signal regions, and compare the observed $\mathrm{E_T^{miss}}$ distribution to the sum of the predictions from the four background categories:

- Z$+$jets background: the $\mathrm{E_T^{miss}}$ in Z$+$jets events is modeled using a data control sample of $\gamma+$jets events. These events are reweighted to account for different jet kinematics in Z$+$jets vs. $\gamma+$jets events using the "$\mathrm{E_T^{miss}}$ templates" technique.
- Flavor-symmetric (FS) background: this background category is dominated by $t\bar{t}$, and consists of processes with equal rates for same-flavor (ee and $\mu\mu$) vs. opposite-flavor (e$\mu$) events. The FS background is predicted from the e$\mu$ data sample. The on-Z dilepton mass requirement is not applied to the e$\mu$ sample, and the predictions are scaled by $K$, the MC efficiency for e$\mu$ background events to satisfy the on-Z dilepton mass requirement.
- WZ/ZZ background: this background is predicted from MC, after validation in 3-lepton (WZ) and 4-lepton (ZZ) data control samples. The contributions from WZ and ZZ to the FS background estimate are negligible.
- Rare background: this background consists of processes with Z bosons ($t\bar{t}$Z and ZZZ, ZZW, ZWW) that have small cross sections, and is estimated from MC.

In order to adapt the $\mathrm{E_T^{miss}}$ templates method to predict the Z background in these regions, we make minor modifications to the procedure used in AN-2012/254. Specifically, we re-calculate the FS scaling factor $K$ and change the binning used for the $\mathrm{E_T^{miss}}$ templates. The details of the extraction of $K$ are presented in App. A; to summarize, we use $K = 0.14 \pm 0.02$ for signal regions with inclusive leptons and $K = 0.15 \pm 0.02$ for signal regions with central leptons. In addition, we change the jet $p_T$ threshold for the $\mathrm{E_T^{miss}}$ templates jet multiplicity binning from 30 to 40 GeV, and change the $H_T$ bins to (0,80,100,150,200,250,300,5000) GeV.

## 4.2 Results in Z Mass Window

The results for the signal regions with inclusive leptons are displayed in Fig. 1 and summarized in Table 3. The results for the signal regions with central leptons are displayed in Fig. 2 and summarized in Table 4. For all four signal regions, the observed $\mathrm{E_T^{miss}}$ distributions agree with the expected $\mathrm{E_T^{miss}}$ distributions for the sum of the backgrounds. The observed yields for the $\mathrm{E_T^{miss}} > 100$ GeV (low-$\mathrm{E_T^{miss}}$) and $\mathrm{E_T^{miss}} > 150$ GeV (high-$\mathrm{E_T^{miss}}$) requirements are consistent with the expected background yields within $\pm 1\sigma$. No evidence of a signal-like excess is observed in any region.

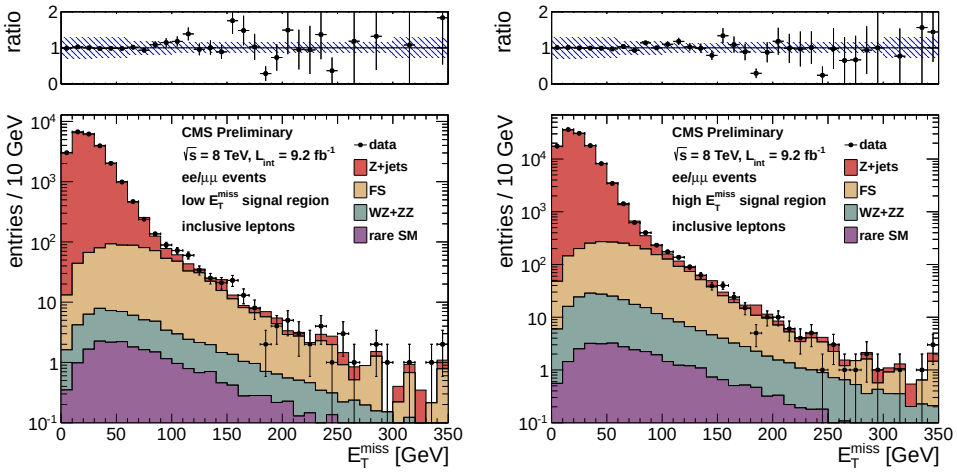


Figure 1: **Results for the low $\mathrm{E_T^{miss}}$ (left) and high $\mathrm{E_T^{miss}}$ (right) signal regions with the inclusive lepton selection.** The observed $\mathrm{E_T^{miss}}$ distribution (black points) is compared with the sum of the predicted $\mathrm{E_T^{miss}}$ distributions from $\mathrm{Z}+\mathrm{jets}$ , flavor-symmetric backgrounds, WZ+ZZ backgrounds, and rare SM backgrounds. The ratio of observed to predicted yields in each bin is indicated. The error bars indicate the statistical uncertainty in the data and the shaded band indicates the total background uncertainty.

Table 3: **Results for $n_{jets} \geq 3$ corresponding to the low $\mathrm{E_T^{miss}}$ signal region (top table) and $n_{jets} \geq 2$ corresponding to the high $\mathrm{E_T^{miss}}$ signal region (bottom table) with the inclusive lepton selection.** The total background is the sum of the $\mathrm{Z}+\mathrm{jets}$ background predicted from the $\mathrm{E_T^{miss}}$ templates method ($\mathrm{Z}+\mathrm{jets}$ bkg), the flavor-symmetric background predicted from e$\mu$ events (FS bkg), the WZ and ZZ backgrounds predicted from MC (WZ bkg and ZZ bkg) and the rare SM backgrounds. All uncertainties include both the statistical and systematic components. The Gaussian significance of the deviation between the data and total background is indicated for signal regions with at least 20 observed events. The numbers in bold correspond to the $\mathrm{E_T^{miss}}$ requirements used to define the low-$\mathrm{E_T^{miss}}$ and high-$\mathrm{E_T^{miss}}$ signal regions.

| | $\mathrm{E_T^{miss}} > 0$ GeV | $\mathrm{E_T^{miss}} > 30$ GeV | $\mathrm{E_T^{miss}} > 60$ GeV | $\mathrm{E_T^{miss}} > 100$ GeV | $\mathrm{E_T^{miss}} > 150$ GeV | $\mathrm{E_T^{miss}} > 300$ GeV |
|---|---|---|---|---|---|---|
| $\mathrm{Z}+\mathrm{jets}$ bkg | $23071 \pm 6922$ | $7456 \pm 2238$ | $673 \pm 203$ | $49.9 \pm 16.4$ | $10.4 \pm 3.6$ | $1.0 \pm 0.6$ |
| FS bkg | $807 \pm 126$ | $695 \pm 108$ | $457 \pm 71$ | $184 \pm 29$ | $45.6 \pm 7.5$ | $1.5 \pm 0.5$ |
| WZ bkg | $43.5 \pm 30.5$ | $35.1 \pm 24.6$ | $21.3 \pm 14.9$ | $10.0 \pm 7.1$ | $4.4 \pm 3.2$ | $0.4 \pm 0.4$ |
| ZZ bkg | $7.8 \pm 3.9$ | $7.0 \pm 3.6$ | $5.4 \pm 2.8$ | $3.3 \pm 1.8$ | $1.7 \pm 1.1$ | $0.2 \pm 0.2$ |
| rare SM bkg | $22.0 \pm 11.0$ | $19.0 \pm 9.6$ | $12.4 \pm 6.3$ | $6.3 \pm 3.3$ | $2.8 \pm 1.6$ | $0.3 \pm 0.3$ |
| total bkg | $23951 \pm 6924$ | $8213 \pm 2241$ | $1169 \pm 216$ | $\mathbf{253 \pm 34}$ | $64.8 \pm 9.1$ | $3.5 \pm 1.0$ |
| data | 23999 | 8134 | 1217 | **288** | 76 | 4 |
| significance | $0.0\sigma$ | $-0.0\sigma$ | $0.2\sigma$ | $\mathbf{0.9}\sigma$ | $0.9\sigma$ | |
| | $\mathrm{E_T^{miss}} > 0$ GeV | $\mathrm{E_T^{miss}} > 30$ GeV | $\mathrm{E_T^{miss}} > 60$ GeV | $\mathrm{E_T^{miss}} > 100$ GeV | $\mathrm{E_T^{miss}} > 150$ GeV | $\mathrm{E_T^{miss}} > 300$ GeV |
| $\mathrm{Z}+\mathrm{jets}$ bkg | $114401 \pm 34322$ | $30966 \pm 9291$ | $1905 \pm 573$ | $120 \pm 38$ | $26.2 \pm 8.9$ | $1.4 \pm 0.7$ |
| FS bkg | $2255 \pm 350$ | $1908 \pm 296$ | $1201 \pm 187$ | $436 \pm 68$ | $90.0 \pm 14.4$ | $2.9 \pm 0.8$ |
| WZ bkg | $182.7 \pm 127.9$ | $144.7 \pm 101.3$ | $81.8 \pm 57.3$ | $35.2 \pm 24.7$ | $13.9 \pm 9.9$ | $1.3 \pm 1.3$ |
| ZZ bkg | $35.9 \pm 18.0$ | $32.3 \pm 16.2$ | $23.9 \pm 12.0$ | $14.0 \pm 7.1$ | $6.7 \pm 3.6$ | $0.8 \pm 0.8$ |
| rare SM bkg | $33.5 \pm 16.8$ | $29.0 \pm 14.6$ | $19.5 \pm 9.8$ | $10.2 \pm 5.2$ | $4.5 \pm 2.5$ | $0.5 \pm 0.5$ |
| total bkg | $116908 \pm 34324$ | $33080 \pm 9296$ | $3231 \pm 605$ | $616 \pm 82$ | $\mathbf{141 \pm 20}$ | $6.9 \pm 1.9$ |
| data | 116978 | 32796 | 3301 | 635 | **133** | 5 |
| significance | $0.0\sigma$ | $-0.0\sigma$ | $0.1\sigma$ | $0.2\sigma$ | $\mathbf{-0.4}\sigma$ | |

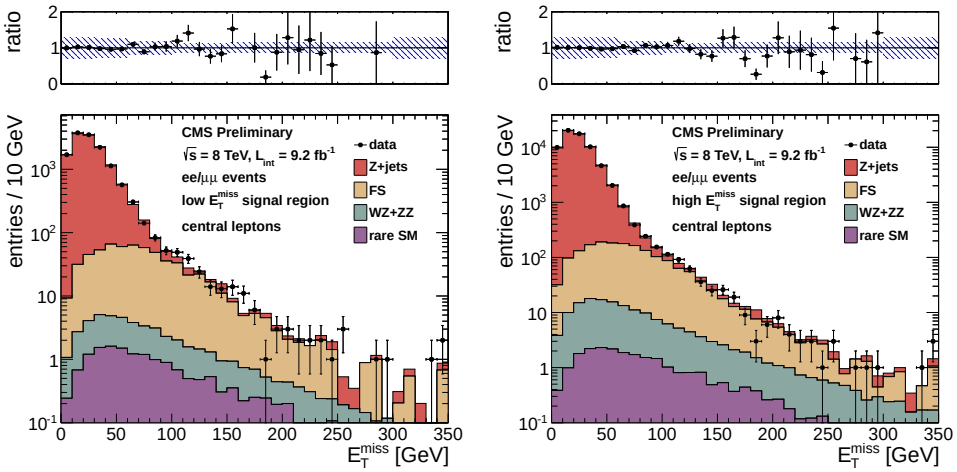


Figure 2: **Results for the low $\mathrm{E_T^{miss}}$ (left) and high $\mathrm{E_T^{miss}}$ (right) signal regions with the central lepton selection.** The observed $\mathrm{E_T^{miss}}$ distribution (black points) is compared with the sum of the predicted $\mathrm{E_T^{miss}}$ distributions from Z + jets , flavor-symmetric backgrounds, WZ+ZZ backgrounds, and rare SM backgrounds. The ratio of observed to predicted yields in each bin is indicated. The error bars indicate the statistical uncertainty in the data and the shaded band indicates the total background uncertainty.

Table 4: **Results for $n_{jets} \geq 3$ corresponding to the low $\mathrm{E_T^{miss}}$ signal region (top table) and $n_{jets} \geq 2$ corresponding to the high $\mathrm{E_T^{miss}}$ signal region (bottom table) with the central lepton selection.** The total background is the sum of the Z + jets background predicted from the $\mathrm{E_T^{miss}}$ templates method (Z + jets bkg), the flavor-symmetric background predicted from e$\mu$ events (FS bkg), the WZ and ZZ backgrounds predicted from MC (WZ bkg and ZZ bkg) and the rare SM backgrounds. All uncertainties include both the statistical and systematic components. The Gaussian significance of the deviation between the data and total background is indicated for signal regions with at least 20 observed events. The numbers in bold correspond to the $\mathrm{E_T^{miss}}$ requirements used to define the low-$\mathrm{E_T^{miss}}$ and high-$\mathrm{E_T^{miss}}$ signal regions.

| | $\mathrm{E_T^{miss}} > 0$ GeV | $\mathrm{E_T^{miss}} > 30$ GeV | $\mathrm{E_T^{miss}} > 60$ GeV | $\mathrm{E_T^{miss}} > 100$ GeV | $\mathrm{E_T^{miss}} > 150$ GeV | $\mathrm{E_T^{miss}} > 300$ GeV |
|---|---|---|---|---|---|---|
| Z + jets bkg | 12984 ± 3896 | 4242 ± 1273 | 391 ± 118 | 29.6 ± 9.7 | 6.3 ± 2.2 | 0.6 ± 0.4 |
| FS bkg | 565 ± 83 | 487 ± 72 | 323 ± 48 | 129 ± 19 | 32.5 ± 5.2 | 1.2 ± 0.5 |
| WZ bkg | 28.1 ± 19.7 | 22.7 ± 15.9 | 13.9 ± 9.8 | 6.8 ± 4.9 | 3.1 ± 2.4 | 0.4 ± 0.4 |
| ZZ bkg | 4.8 ± 2.5 | 4.4 ± 2.3 | 3.3 ± 1.8 | 2.1 ± 1.2 | 1.1 ± 0.8 | 0.1 ± 0.1 |
| rare SM bkg | 15.8 ± 8.0 | 13.7 ± 6.9 | 9.0 ± 4.6 | 4.8 ± 2.5 | 2.3 ± 1.4 | 0.3 ± 0.3 |
| total bkg | 13598 ± 3897 | 4770 ± 1275 | 740 ± 128 | **173 ± 22** | 45.2 ± 6.3 | 2.6 ± 0.7 |
| data | 13631 | 4688 | 773 | **192** | 53 | 3 |
| significance | 0.0$\sigma$ | -0.1$\sigma$ | 0.3$\sigma$ | **0.7**$\sigma$ | 0.8$\sigma$ | |

| | $\mathrm{E_T^{miss}} > 0$ GeV | $\mathrm{E_T^{miss}} > 30$ GeV | $\mathrm{E_T^{miss}} > 60$ GeV | $\mathrm{E_T^{miss}} > 100$ GeV | $\mathrm{E_T^{miss}} > 150$ GeV | $\mathrm{E_T^{miss}} > 300$ GeV |
|---|---|---|---|---|---|---|
| Z + jets bkg | 64775 ± 19433 | 17697 ± 5310 | 1118 ± 336 | 71.8 ± 22.3 | 15.8 ± 5.3 | 0.8 ± 0.4 |
| FS bkg | 1573 ± 231 | 1341 ± 197 | 850 ± 125 | 313 ± 46 | 66.5 ± 10.2 | 2.2 ± 0.7 |
| WZ bkg | 115.0 ± 80.5 | 91.3 ± 64.0 | 52.4 ± 36.7 | 23.3 ± 16.4 | 9.4 ± 6.7 | 1.0 ± 1.0 |
| ZZ bkg | 21.7 ± 10.9 | 19.7 ± 9.9 | 14.8 ± 7.5 | 8.8 ± 4.5 | 4.3 ± 2.4 | 0.5 ± 0.5 |
| rare SM bkg | 23.9 ± 12.0 | 20.8 ± 10.4 | 14.1 ± 7.1 | 7.5 ± 3.9 | 3.6 ± 2.1 | 0.5 ± 0.5 |
| total bkg | 66508 ± 19435 | 19170 ± 5314 | 2049 ± 360 | 424 ± 54 | **99.6 ± 13.7** | 5.1 ± 1.4 |
| data | 66521 | 18841 | 2062 | 421 | **92** | 4 |
| significance | 0.0$\sigma$ | -0.1$\sigma$ | 0.0$\sigma$ | -0.1$\sigma$ | **-0.5**$\sigma$ | |

### 4.3 Extrapolation to Low Mass to Estimate the $\gamma^*/Z$ Contribution

Given a prediction for the Z background in the Z mass window, we can extrapolate to estimate the low mass $\gamma^*$/Z contribution. We extract the ratio $\mathrm{R_{low/in}}$ of low-mass to on-shell Z events from data, correcting for the contribution from flavor-symmetric backgrounds, according to:

$$R_{low/in} = (N_{SF}^{low} - N_{OF}^{low})/(N_{SF}^{in} - N_{OF}^{in}). \quad (1)$$

Here SF and OF refer to the same-flavor and opposite-flavor data yields in the "low" ($20 < m_{\ell\ell} < 70$ GeV) and "in" ($81 < m_{\ell\ell} < 101$ GeV) dilepton mass regions. To predict the low-mass $\gamma^*$/Z contribution, we scale the total predicted Z background by this quantity. The measurement of $\mathrm{R_{low/in}}$ is summarized in App. B; to summarize, we find $\mathrm{R_{low/in}} = 0.07 \pm 0.02$.

To predict the low-mass $\gamma^*$/Z background, we start with the prediction for the total Z background in the on-Z regions for the four signal regions (see the bold numbers from Tables 3 and 4). Here the total Z background is the sum of $\mathrm{Z} + \mathrm{jets}$ , WZ, ZZ, and rare SM backgrounds. This background is then scaled by $\mathrm{R_{low/in}}$ to predict the $\gamma^*$/Z contribution to the low-mass region of the four signal regions. The results are summarized in Table 5.

# 5 Summary of Results

Assummary of the results in presented in Table 5. The observed data yields in the on-Z regions for the four signal regions (low-$\mathrm{E_T^{miss}}$ and high-$\mathrm{E_T^{miss}}$, inclusive and central leptons) are in good agreement with the predicted backgrounds. The last 2 rows of Table 5 present the total Z background in the on-Z region, and the extrapolation to the low-mass region.

The Z background predictions in the on-Z region are compared with the corresponding predictions from the JZB method in Table 6. The predictions are consistent in all four signal regions.

Table 5: Summary of results in the four signal regions. The total observed yields in the on-Z regions (Total On-Z Yield) is compared to the total predicted background in the on-Z region (Total On-Z Bkg). The total Z background (sum of $\mathrm{Z} + \mathrm{jets}$ , WZ, ZZ, and rare SM backgrounds) in the on-Z region is indicated (On-Z Z Bkg). This Z background is scaled by $\mathrm{R_{low/in}} = 0.07 \pm 0.02$ to predict the $\gamma^*$/Z contribution to the low-mass region ($\gamma^*$/Z Bkg).

| | Low-$\mathrm{E_T^{miss}}$ (central) | Low-$\mathrm{E_T^{miss}}$ (inclusive) | High-$\mathrm{E_T^{miss}}$ (central) | High-$\mathrm{E_T^{miss}}$ (inclusive) |
|---|---|---|---|---|
| Total On-Z Yield | 192 | 288 | 92 | 133 |
| Total On-Z Bkg | $173 \pm 22$ | $253 \pm 34$ | $100 \pm 14$ | $141 \pm 20$ |
| On-Z Z Bkg | $43 \pm 11$ | $70 \pm 18$ | $33 \pm 9.1$ | $51 \pm 14$ |
| $\gamma^*$/Z Bkg | $3.0 \pm 1.2$ | $4.9 \pm 1.9$ | $2.3 \pm 0.9$ | $3.6 \pm 1.4$ |

Table 6: Comparison of the Z background predictions in the on-Z region obtained with the $\mathrm{E_T^{miss}}$ templates and JZB methods.

| | Low $\mathrm{E_T^{miss}}$ | | High $\mathrm{E_T^{miss}}$ | |
|---|---|---|---|---|
| | central | inclusive | central | inclusive |
| JZB | $32 \pm 8 \pm 6.4$ | $45 \pm 9 \pm 9$ | $24 \pm 6.9 \pm 7.2$ | $30 \pm 8 \pm 9$ |
| $\mathrm{E_T^{miss}}$ templates | $43 \pm 11$ | $70 \pm 18$ | $33 \pm 9.1$ | $51 \pm 14$ |

# References


[1] CMS Collaboration, "Search for physics beyond the standard model in events with a Z boson, jets, and missing transverse energy in pp collisions at $\sqrt{s} = 7$ TeV,", arXiv:1204.3774v1 [hep-ex].

[2] CMS AN-2009/023. "A Method to Measure the Contribution of DY$\rightarrow \ell^+\ell$ to a dilepton + $\mathrm{E_T^{miss}}$ Selection."

# A Measurement of K

To measure the flavor-symmetric background (mostly $t\bar{t}$) in the Z mass window, we take the e$\mu$ yield without the on-Z mass requirement and scale this by the quantity K, which is the MC efficiency for the flavor-symmetric background to fall in the Z mass window. In this section we measure K from MC for the high-$\mathrm{E_T^{miss}}$ and low-$\mathrm{E_T^{miss}}$ signal regions, for central and inclusive leptons. The measurement is made in various $\mathrm{E_T^{miss}}$ regions, and the uncertainty is assessed based on comparison of K with the corresponding value extracted from data.

The values of K for the high-$\mathrm{E_T^{miss}}$ signal region are in Fig. 3 (inclusive leptons) and Fig. 4 (central leptons). The values of K for the low-$\mathrm{E_T^{miss}}$ signal region are in Fig. 5 (inclusive leptons) and Fig. 6 (central leptons).

For the inclusive leptons, we find that $K = 0.14 \pm 0.02$ for all $\mathrm{E_T^{miss}}$ regions up to $\mathrm{E_T^{miss}} > 150$ GeV (the largest $\mathrm{E_T^{miss}}$ requirement used in the edge analysis) For the central leptons, we find $K = 0.15 \pm 0.02$.

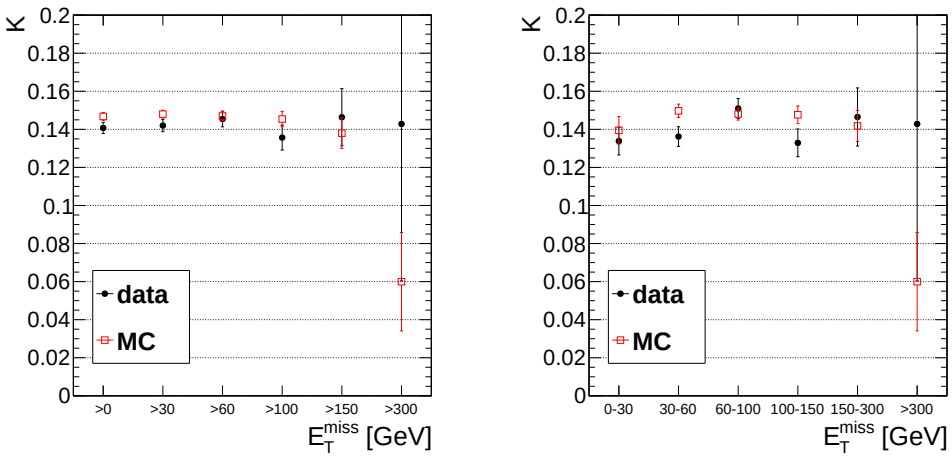


Figure 3: The efficiency for e$\mu$ events to satisfy the dilepton mass requirement, $K$, in data and simulation for inclusive $\mathrm{E_T^{miss}}$ intervals (left) and exclusive $\mathrm{E_T^{miss}}$ intervals (right) for the **high-$\mathrm{E_T^{miss}}$ signal region requirements and inclusive leptons**.

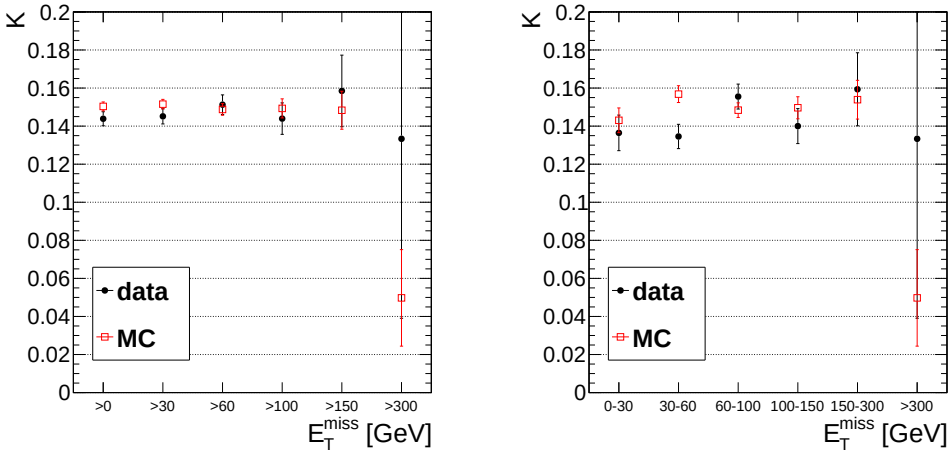


Figure 4: The efficiency for e$\mu$ events to satisfy the dilepton mass requirement, $K$, in data and simulation for inclusive $\mathrm{E_T^{miss}}$ intervals (left) and exclusive $\mathrm{E_T^{miss}}$ intervals (right) for the **high-$\mathrm{E_T^{miss}}$ signal region requirements and central leptons**.

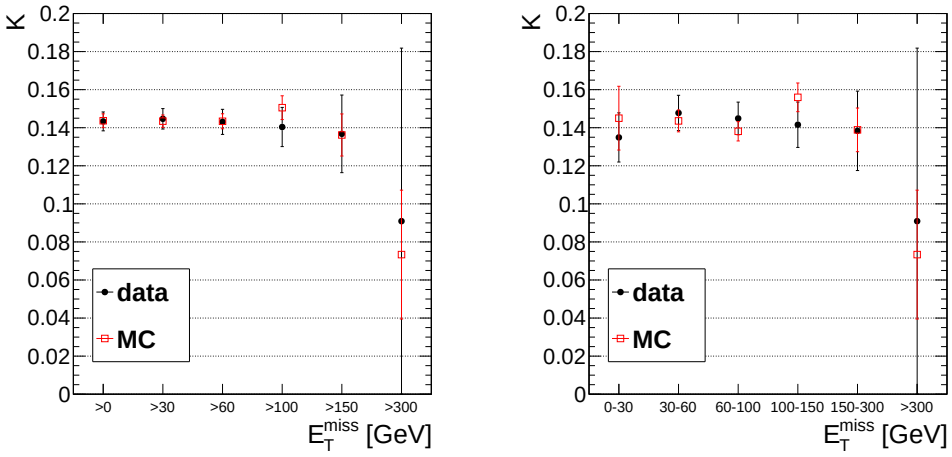


Figure 5: The efficiency for e$\mu$ events to satisfy the dilepton mass requirement, $K$, in data and simulation for inclusive $\mathrm{E_T^{miss}}$ intervals (left) and exclusive $\mathrm{E_T^{miss}}$ intervals (right) for the **low-$\mathrm{E_T^{miss}}$ signal region requirements and inclusive leptons**.

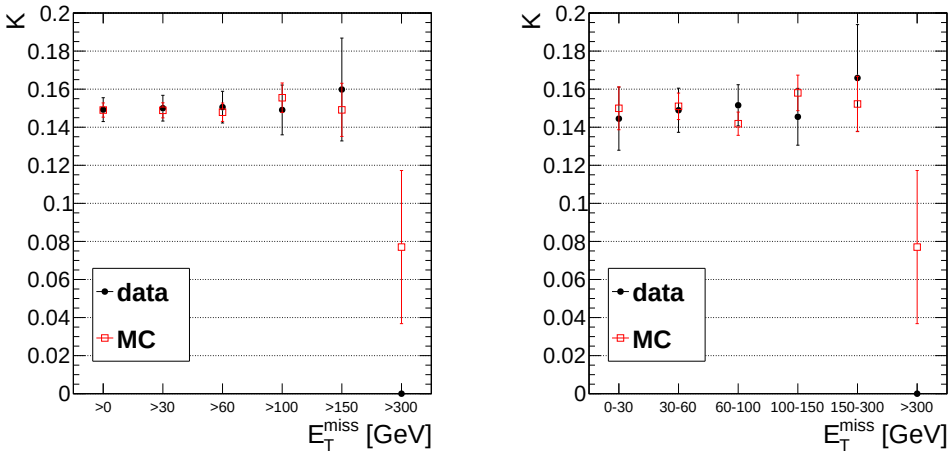


Figure 6: The efficiency for e$\mu$ events to satisfy the dilepton mass requirement, $K$, in data and simulation for inclusive $\mathrm{E_T^{miss}}$ intervals (left) and exclusive $\mathrm{E_T^{miss}}$ intervals (right) for the **low-$\mathrm{E_T^{miss}}$ signal region requirements and central leptons**.

# B Measurement of $\mathrm{R_{low/in}}$

The Z background in the on-Z region is extrapolated to predict the $\gamma*$/Z background in the low-mass background using the extrapolation factor $\mathrm{R_{low/in}}$ discussed in Sec. 4. In this section we measure $\mathrm{R_{low/in}}$ , as a function of $\mathrm{E_T^{miss}}$, for the jet and lepton requirements corresponding to the low-$\mathrm{E_T^{miss}}$ and high-$\mathrm{E_T^{miss}}$ signal regions, with inclusive and central leptons.

The values of $\mathrm{R_{low/in}}$ for the high-$\mathrm{E_T^{miss}}$ signal region are in Fig. 7. The values of $\mathrm{R_{low/in}}$ for the low-$\mathrm{E_T^{miss}}$ signal region are in Fig. 8. For all signal regions, we find $\mathrm{R_{low/in}} = 0.07 \pm 0.02$.

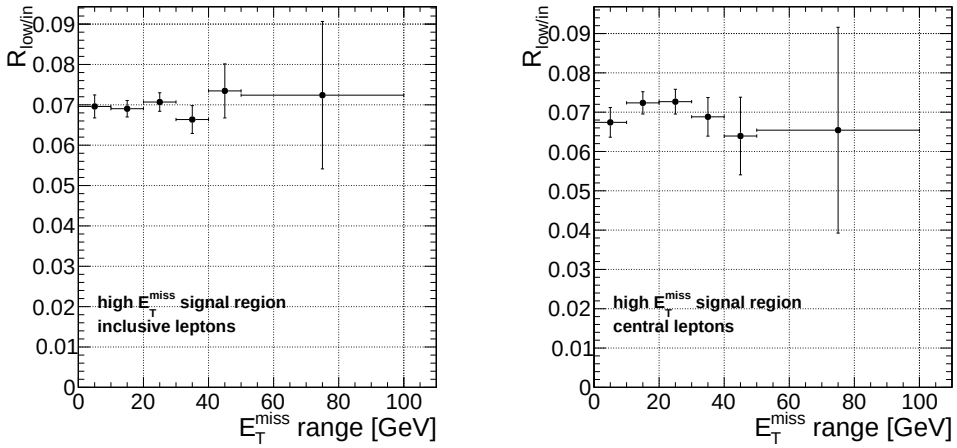


Figure 7: The quantity $\mathrm{R_{low/in}}$ for the high-$\mathrm{E_T^{miss}}$ signal region with inclusive leptons (left) and central leptons (right).

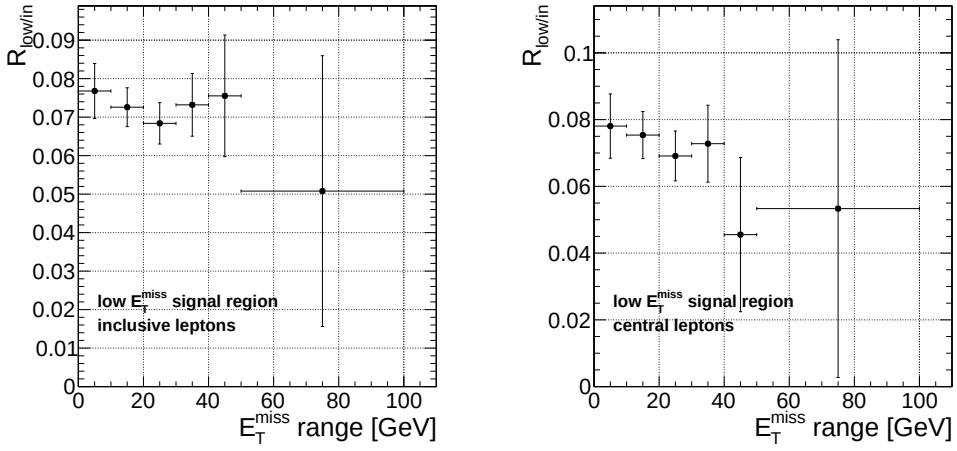


Figure 8: The quantity $\mathrm{R_{low/in}}$ for the low-$\mathrm{E_T^{miss}}$ signal region with inclusive leptons (left) and central leptons (right).

# C Cross-check with single lepton triggers

**The results in this section are based on the old definitions of the high-$\mathrm{E_T^{miss}}$ and low-$\mathrm{E_T^{miss}}$ signal regions. The high-$\mathrm{E_T^{miss}}$ signal region has $p_T$ > (20,10) GeV leptons. The low-$\mathrm{E_T^{miss}}$ signal region has inclusive leptons.** The nominal "edge analysis" is performed with dilepton triggers. An excess of SF vs. OF events may thus be observed if there were some inefficiency for the e$\mu$ triggers used in this analysis. In this section we provide a cross-check of the nominal analysis by including events collected with single lepton triggers. The relevant triggers are:

- ee channel
  - dilepton: `HLT_Ele17_CaloIdT_CaloIsoVL_TrkIdVL_TrkIsoVL_Ele8_CaloIdT_CaloIsoVL_TrkIdVL_TrkIsoVL`
  - single lepton: `HLT_Ele27_WP80`
- $\mu\mu$ channel
  - dilepton: `HLT_Mu17_Mu8` OR `HLT_Mu17_TkMu8`
  - single lepton: `HLT_IsoMu24` OR `HLT_IsoMu24_eta2p1`
- $e\mu$ channel
  - dilepton: `HLT_MuX_EleY_CaloIdT_CaloIsoVL_TrkIdVL_TrkIsoVL` (X,Y=17,8 OR 8,17)
  - single lepton: `HLT_Ele27_WP80` OR `HLT_IsoMu24` OR `HLT_IsoMu24_eta2p1`

In the nominal analysis based on dilepton triggers only, an ee event is required to satisfy the ee dilepton trigger, a $\mu\mu$ event is required to satisfy one of the two $\mu\mu$ dilepton triggers, and an e$\mu$ event is required to satisfy one of the two e$\mu$ dilepton triggers. Here we compare the results obtained from the nominal dilepton triggers with those obtained by requiring an OR of the dilepton and single lepton triggers. In this cross-check, an ee event is required to satisfy the ee dilepton trigger OR single electron trigger, a $\mu\mu$ event is required to satisfy one of the two $\mu\mu$ dilepton triggers OR one of the two single muon triggers, and an e$\mu$ event is required to satisfy one of the two e$\mu$ dilepton triggers OR the single electron trigger OR the single muon trigger. The results are summarized in Table 7. Including the single lepton triggers increases the yields in the ee, $\mu\mu$ and e$\mu$ final states by (1–7)%, and does not significantly alter the excess of SF vs. OF data yields.

Table 7: Summary of results comparing dilepton vs. dilepton OR single lepton triggers, for 5.1 fb$^{-1}$, in the low $\mathrm{E_T^{miss}}$ and high $\mathrm{E_T^{miss}}$ signal regions (SR). The ratio of the dilepton OR single lepton yield to the dilepton only yield is indicated, along with the excess of SF w.r.t. OF events.

| Region | $N_{\mathrm{ee}}$ | $N_{\mu\mu}$ | $N_{\mathrm{e}\mu}$ | $N_{\mathrm{ee}} + N_{\mu\mu} - N_{\mathrm{e}\mu}$ |
|---|---|---|---|---|
| Low $\mathrm{E_T^{miss}}$ SR and $20 < m_{\ell\ell} < 70$ GeV | | | | |
| dilepton (nominal) | 106 | 153 | 189 | $70 \pm 21.2$ (stat) |
| dilepton OR single lepton | 112 | 155 | 199 | $68 \pm 21.6$ (stat) |
| ratio | 1.06 | 1.01 | 1.05 | |
| Low $\mathrm{E_T^{miss}}$ SR and $m_{\ell\ell} > 20$ GeV | | | | |
| dilepton (nominal) | 357 | 517 | 693 | $181 \pm 39.6$ (stat) |
| dilepton OR single lepton | 368 | 534 | 739 | $163 \pm 40.5$ (stat) |
| ratio | 1.03 | 1.03 | 1.07 | |
| High $\mathrm{E_T^{miss}}$ SR and $15 < m_{\ell\ell} < 70$ GeV | | | | |
| dilepton (nominal) | 89 | 157 | 187 | $59 \pm 20.8$ (stat) |
| dilepton OR single lepton | 93 | 160 | 197 | $56 \pm 21.2$ (stat) |
| ratio | 1.04 | 1.02 | 1.05 | |
| High $\mathrm{E_T^{miss}}$ SR and $m_{\ell\ell} > 15$ GeV | | | | |
| dilepton (nominal) | 258 | 380 | 527 | $111 \pm 34.1$ (stat) |
| dilepton OR single lepton | 271 | 386 | 553 | $104 \pm 34.8$ (stat) |
| ratio | 1.05 | 1.02 | 1.05 | |

Next, we compare the results obtained with the dilepton triggers to results obtained with single lepton triggers only. Since the single electron (single muon) triggers have $p_T$ thresholds of 27 (24) GeV, we use a dilepton $p_T >$ (30,20) selection. The results are summarized in Table 8. Switching from dilepton to single lepton triggers alters the yields by (-2–5)%, and does not significantly alter the excess of SF vs. OF data yields.

Table 8: Summary of results comparing dilepton vs. single lepton triggers (with a dilepton $p_T >$ (30,20) GeV selection, for 5.1 fb$^{-1}$, in the low $\mathrm{E_T^{miss}}$ and high $\mathrm{E_T^{miss}}$ signal regions (SR). The ratio of the single lepton trigger yield to the dilepton trigger yield is indicated, along with the excess of SF w.r.t. OF events.

| Region | $N_{\mathrm{ee}}$ | $N_{\mu\mu}$ | $N_{\mathrm{e}\mu}$ | $N_{\mathrm{ee}} + N_{\mu\mu} - N_{\mathrm{e}\mu}$ |
|---|---|---|---|---|
| Low $\mathrm{E_T^{miss}}$ SR and $20 < m_{\ell\ell} < 70$ GeV | | | | |
| dilepton | 95 | 135 | 169 | 61 $\pm$ 20.0 (stat) |
| single lepton | 93 | 134 | 172 | 55 $\pm$ 20.0 (stat) |
| ratio | 0.98 | 0.99 | 1.02 | |
| Low $\mathrm{E_T^{miss}}$ SR and $m_{\ell\ell} > 20$ GeV | | | | |
| dilepton | 345 | 497 | 669 | 173 $\pm$ 38.9 (stat) |
| single lepton | 346 | 499 | 700 | 145 $\pm$ 39.3 (stat) |
| ratio | 1.00 | 1.00 | 1.05 | |
| High $\mathrm{E_T^{miss}}$ SR and $15 < m_{\ell\ell} < 70$ GeV | | | | |
| dilepton | 48 | 72 | 79 | 41 $\pm$ 14.1 (stat) |
| single lepton | 47 | 72 | 81 | 38 $\pm$ 14.1 (stat) |
| ratio | 0.98 | 1.00 | 1.03 | |
| High $\mathrm{E_T^{miss}}$ SR and $m_{\ell\ell} > 15$ GeV | | | | |
| dilepton | 197 | 270 | 367 | 100 $\pm$ 28.9 (stat) |
| single lepton | 200 | 269 | 377 | 92 $\pm$ 29.1 (stat) |
| ratio | 1.02 | 1.00 | 1.03 | |